Mathl. Comput. Modelling Vol. 17, No. 8, pp. 11–22, 1993
Printed in Great Britain

0895-7177/93 $6.00 + 0.00
Pergamon Press Ltd

TRAFFIC FLOW SIMULATION THROUGH HIGH ORDER TRAFFIC MODELLING

A. CHRONOPOULOS, A. LYRINTZIS, P. MICHALOPOULOS, C. RHEE AND P. YI
University of Minnesota—Twin Cities
200 Union Street S.E., Minneapolis, MN 55455, U.S.A.

(Received October 1992; accepted November 1992)

Abstract—Explicit and implicit numerical methods for solving simple traffic flow continuum models have been studied and efficiently implemented in traffic simulation codes. We studied and implemented explicit and implicit numerical methods for solving high-order flow conservation traffic models. The acceleration and inertia effects of the traffic mass are properly addressed in the new formulations. The high order model does not employ equilibrium flow-density relationships. We wrote an experimental code in C to simulate a freeway (un)congested pipeline and freeway entry/exit traffic flow. Tests with real data collected from the I-35 W freeway in Minneapolis were conducted on a workstation computer. The implicit Euler method gave the same (and in some cases better) accuracy as the explicit Lax method. The implicit Euler method was (about three times) faster than the Lax method.

1. INTRODUCTION

Continuum traffic flow models based on traffic density, flow, and velocity have been proposed and analyzed in the past. Examples include Lighthill and Whitham's [1] flow conservation model, Payne's momentum conservation model [2], and Michalopoulos's momentum model [3]. These models involve partial differential equations (PDEs) defined on appropriate domains with suitable boundary conditions which describe various traffic phenomena and road geometries.

The improvement of computational efficiency in the continuum traffic models has been the focal point in the development of traffic simulation programs. It is understood that the computer execution time to solve traffic flow problems depends not only on the size of the freeway and the complexity of roadway geometries, but also on the model equations and numerical schemes used in their discretization.

Explicit numerical methods (for example Lax, Upwind) have been used by Michalopoulos and Lin and Leo and Pretty to compute the solution of the simple traffic flow continuum models [4,5]. In these explicit schemes, the space and time mesh sizes are restricted both by accuracy and numerical stability requirements. In order to reduce the computer execution time and maintain good accuracy, the total number of computations must be reduced. This can be achieved by using larger values of time and space mesh sizes. Implicit numerical methods provide the same accuracy as explicit methods and allow changes in the mesh sizes while maintaining numerical stability [6,7].

In this work, we use implicit numerical method (Backward Euler) to solve more efficiently the momentum conservation model. We wrote an experimental code in C simulating a freeway (un)congested pipeline and freeway entry/exit traffic flow. Tests with real data collected from the I-35 W freeway in Minneapolis were conducted. These data have been collected by the Department of Civil Engineering at the University of Minnesota and the Minnesota Department

The first four authors are at the University of Minnesota and the last author is at MN/DOT. A. Chronopoulos is an assistant professor at the Computer Science Dept., A. Lyrintzis is an assistant professor at the Dept. of Aerospace Engineering and Mechanics, P. Michalopoulos is a professor at the Civil and Mineral Engineering Dept. C. Rhee is a Master's student in Computer Science and P. Yi is a researcher at the Minnesota Department of Transportation. This work was supported by the University of Minnesota Center of Transportation Studies.

Typeset by $\mathcal{A}_{\mathcal{M}}\mathcal{S}$-TEX

of Transportation. Using these data, we tested (for accuracy and efficiency) the implicit Euler method against the Lax method on a Sun Sparc1 workstation computer. The implicit Euler method yielded the same (or better accuracy) as the Lax method and it was (about three times) faster than the Lax method.

The outline of this article is as follows. In Section 2, we review the momentum conservation continuum traffic model. In Section 3, we review the Euler implicit and Lax methods. In Section 4, we describe the congested/uncongested and entry/exit freeway models. In Section 5, we present the numerical results. Section 6 contains concluding remarks.

2. A SIMPLE AND HIGH-ORDER CONTINUUM MODEL OF TRAFFIC FLOW

The following conservation equation has been proposed by Lighthill and Whitham [1] as a simple continuum traffic model:

$$\frac{\partial k}{\partial t} + \frac{\partial q}{\partial x} = g(x,t), \tag{1}$$

where $k(x,t)$ and $q(x,t)$ are the traffic density and flow, respectively, at the space-time point (x,t). The generation term $g(x,t)$ represents the number of cars entering or leaving the traffic flow in a freeway with entries/exits. The traffic flow, density, and speed are related by the equation

$$q = ku, \tag{2}$$

where the equilibrium speed $u(x,t) = u(k)$ must be provided by a theoretical or empirical u-k model. The theoretical u-k model, equation of state, can take the general form

$$u_e = u_f \left[1 - \left(\frac{k}{k_{\text{jam}}}\right)^{\alpha}\right]^{\beta}, \tag{3}$$

where u_f is the free flow speed and k_{jam} the jam density [8]. For instance, for $\alpha = 1$ and $\beta = 1$, one obtains the Greenshield's [8] equation of state. More information on this and other forms of the u-k relationships can be found elsewhere [9]. Since the simple continuum model does not consider acceleration and inertia effects, it does not faithfully describe non-equilibrium traffic flow dynamics.

The high-order continuum formulation takes into account acceleration and inertia effects by replacing equation (3) with a momentum equation. For example, the equation in [3] has the following form:

$$\frac{du}{dt} = \frac{1}{T}[u_f(x) - u] - G\frac{\partial u}{\partial t} - \nu k^{\beta}\frac{\partial k}{\partial x}, \tag{4}$$

where $\frac{du}{dt}$ is the acceleration of an observer moving with the traffic stream and is related to the acceleration $\frac{\partial u}{\partial t}$ of the traffic stream as seen by an observer at a fixed point of the road, i.e.,

$$\frac{du}{dt} = \frac{\partial u}{\partial t} + u\frac{\partial u}{\partial x}. \tag{5}$$

The first term on the right hand side of equation (4), $1/T\,[u_f(x) - u]$, represents the relaxation term, the tendency of traffic flow to adjust speeds due to changes in in free-flow speed $u_f(x)$ along the roadway, where relaxation time T is assumed to vary with density k according to

$$T = t_0\left(1 + \frac{rk}{k_{\text{jam}} - rk}\right), \tag{6}$$

where $t_0 > 0$ and $0 < r < 1$ are constants. The second term, $G\frac{\partial u}{\partial t}$, addresses the traffic friction at freeway ramp junctions due to ramp flows. G is the friction parameter. It is a function of both roadway conditions and the ramp volume entering or leaving the freeway and is derived experimentally as $G = \mu k^{\epsilon} g$, where μ is a geometry parameter depending on the type of road geometry, ϵ is a dimensionless constant, and g is the generation term. The third term, $\nu k^{\beta}\frac{\partial k}{\partial x}$, represents the anticipation term which is the effect of drivers reacting to downstream traffic conditions. In this term ν is the anticipation parameter. As implied in this example, if downstream density is higher due to congestion, speed has to be decreased accordingly. Conversely, if downstream density is lower, speed can be increased. From equations (4)–(6), one derives a momentum model for the traffic flow described by the following system of PDEs:

$$\frac{\partial \vec{\mathbf{U}}}{\partial \mathrm{t}} + \frac{\partial \vec{\mathbf{E}}}{\partial \mathrm{x}} = \vec{\mathbf{Z}}, \tag{7}$$

where $\vec{U}$, $\vec{E}$, and $\vec{Z}$ are the following vectors:

$$\vec{U} = \begin{pmatrix} k \\ q \end{pmatrix},$$

$$\vec{E} = \begin{pmatrix} ku \\ u^2 k + \frac{\nu}{\beta+2} k^{\beta+2} \end{pmatrix},$$

$$\vec{Z} = \begin{pmatrix} g \\ \frac{k}{T}[u_f(x) - u] - Gk\frac{\partial u}{\partial t} \end{pmatrix}.$$

We note that the momentum conservation model does not require a q-k curve as in the case of the simple continuum model. In our implementation, we neglected the traffic friction (i.e., we set $G = 0$ in (4)).

3. NUMERICAL METHODS

We consider one explicit method (Lax) and one implicit method (Euler implicit) which are used in computational fluid dynamics [6]. For each traffic model, the road section (the space dimension) is discretized using uniform mesh for all numerical methods; only the time stepsizes differ between methods. We use the following notation:

$\Delta t =$ time stepsize.
$\Delta x =$ space stepsize.
$k_j^n =$ density (vehicles/mile/lane) at space node $j\Delta x$ and at time $n\Delta t$.
$q_j^n =$ flow (vehicles/hour/lane) at space node $j\Delta x$ and at time $n\Delta t$.
$u_j^n =$ speed (mile/hour) at space node $j\Delta x$ and at time $n\Delta t$.

3.1. Lax Method

The Lax method is an explicit method. The new density value k_j^{n+1} and flow value q_j^{n+1} are computed directly from the density and flow at the preceding time step n:

$$\vec{U}_j^{n+1} = \frac{\vec{U}_{j+1}^n + \vec{U}_{j-1}^n}{2} - \frac{\Delta t}{\Delta x}\frac{\vec{E}_{j+1}^n - \vec{E}_{j-1}^n}{2} + \frac{\Delta t}{2}(\vec{Z}_{j+1}^n + \vec{Z}_{j-1}^n). \tag{8}$$

The method is of first order accuracy with respect to Δt, i.e., the error is $O(\Delta t)$. To maintain numerical stability, time and space stepsizes must satisfy the CFL condition $\frac{\Delta x}{\Delta t} > u_f$, where u_f is the free flow speed. For example, in the KRONOS [10] traffic simulation code (using Lax) $\Delta x = 100$ feet and $\Delta t = 1$ sec are recommended.

3.2. Euler Implicit

The Euler implicit method applied to the nonlinear PDE (1) generates a nonlinear recursion involving all space nodes at each time step. To solve numerically this recursion, Beam and Warming have suggested using Newton linearization steps [6]. Each Newton step constructs a linear system of the banded matrix with unknowns $\Delta\vec{U}_j = \vec{U}_j^{n+1} - \vec{U}_j^n$.

$$-\frac{\Delta t}{2\Delta x}\left(\frac{\partial \vec{E}}{\partial \vec{U}}\right)_{j-1}^n \Delta\vec{U}_{j-1} + \left[1 - \Delta t\left(\frac{\partial \vec{Z}}{\partial \vec{U}}\right)_j^n\right]\Delta\vec{U}_j + \frac{\Delta t}{2\Delta x}\left(\frac{\partial \vec{E}}{\partial \vec{U}}\right)_{j+1}^n \Delta\vec{U}_{j+1} = -\frac{\Delta t}{2\Delta x}\left(\vec{E}_{j+1}^n - \vec{E}_{j-1}^n\right) + \Delta t\left(\frac{\partial \vec{Z}}{\partial \vec{U}}\right)_j^n \vec{U}_j^n$$

where

$$\left(\frac{\partial \vec{E}}{\partial \vec{U}}\right)_j^n = \begin{pmatrix} 0 & 1 \\ -u^2+\nu & 2\frac{q}{k} \end{pmatrix}_j^n$$

$$\left(\frac{\partial \vec{Z}}{\partial \vec{U}}\right)_j^n = \begin{pmatrix} 0 & 0 \\ \frac{u_f}{t_0 k_{\text{jam}}}\left(k_{\text{jam}} - 2rk\right) + \frac{r}{t_0 k_{\text{jam}}} q & -\frac{k_{\text{jam}} - rk}{t_0 k_{\text{jam}}} \end{pmatrix}_j^n$$

This linear system of banded matrix is solved by the band Gaussian elimination method with partial pivoting. The LINPACK Fortran subroutines were called upon by a C program driver to solve the above linear system [11]. The solution is then advanced to the next time step simultaneously at all space nodes by computing $\vec{U}_j^{n+1} = \vec{U}_j^n + \Delta\vec{U}_j$. This method is of first order accuracy with respect to Δt. However, its main advantage that it is unconditionally stable.

Artificial smoothing is often added to reduce oscillatory behavior in the numerical solution. This is achieved by adding a fourth order damping term d_j to each term $\vec{U}_j$

$$d_j = -\frac{\omega}{8}\left(\vec{U}_{j-2} - 4\vec{U}_{j-1} + 6\vec{U}_j - 4\vec{U}_{j+1} + \vec{U}_{j+2}\right).$$

We have tested several damping coefficients with ω ranging from $\omega = 0$ (no damping) to $\omega = 1$. The choice $\omega = 1$ gave the best results.

The Euler implicit method requires the computation of the Jacobians $\frac{\partial \vec{E}}{\partial \vec{U}}$ and $\frac{\partial \vec{Z}}{\partial \vec{U}}$. This method involves more computations per time step than Lax. However, Euler implicit method allows much larger stepsizes which make the overall computer execution time less than that of the Lax method.

4. FREEWAY TRAFFIC MODEL CASES

Three freeway traffic flow cases were used to test the numerical methods described above. Each case consists of a section of a single-lane freeway, where the data sets used give the number of vehicles counted crossing each boundary during each 5-minute interval, and then are multiplied by 12 and divided by the number of lanes to yield an average single-lane flow rate in vehicles/hour/lane. The field data are collected as follows: a detector is placed at a *check station* which counts the volume of cars passing that road point every 5 minutes. Check stations are set at the upstream and downstream boundaries and at one or more locations in the freeway stretch in between. In the (un)congested pipeline cases, speed was not available from our data. We used a piecewise linear q-k curve [7] to compute the speed values only at the upstream and downstream boundary.

4.1. Uncongested Pipeline

The uncongested pipeline freeway traffic case consisted of a 4000-ft segment of a two lane freeway. In this case, the road segment contains no entry or exit ramps and the traffic flow is always uncongested. This was the Minneapolis I-35 W northbound between 76th and 70th Streets with a check station located at 73rd Street. The roadway geometry for the uncongested pipeline case is presented in Figure 1. The arrival and departure pattern for the uncongested pipeline is shown in Figure 4. Observations were recorded at 5-minute intervals over a span of 2 hours. These field data have also been used in [3,7,10].

4.2. Congested Pipeline

The congested pipeline case allows both congested and uncongested flow in a road segment without entry or exit ramps. The data set used in this case was taken from observations of a 3600 ft segment of four lane freeway. This was the Minneapolis I-35 W southbound between 26th and 31st Streets with a check station at 28th Street. Then the traffic flow measurements (vehicles/5 minutes/4 lanes) were made at the upstream and downstream boundaries and at a check station point 1600 ft from the upstream boundary. Along with the flow measurements, the state of congestion (uncongested or congested) at the boundaries was also recorded. The roadway geometry for the congested pipeline case is presented in Figure 2. The arrival and

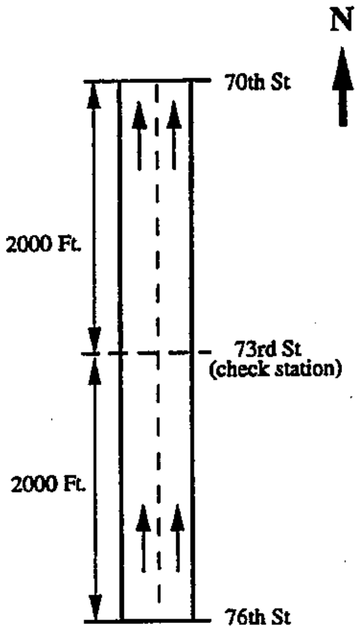

Figure 1. Roadway geometry for uncongested pipeline case.

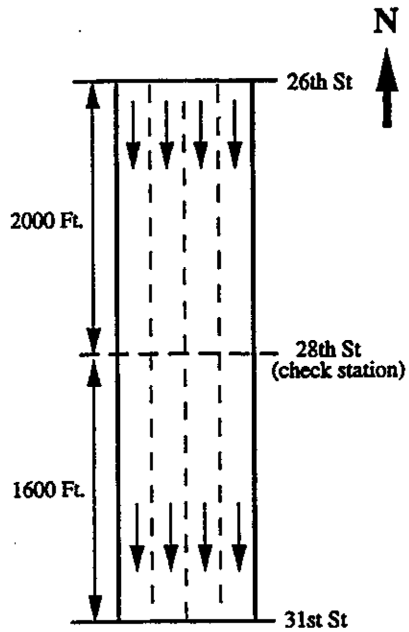

Figure 2. Roadway geometry for congested pipeline case.

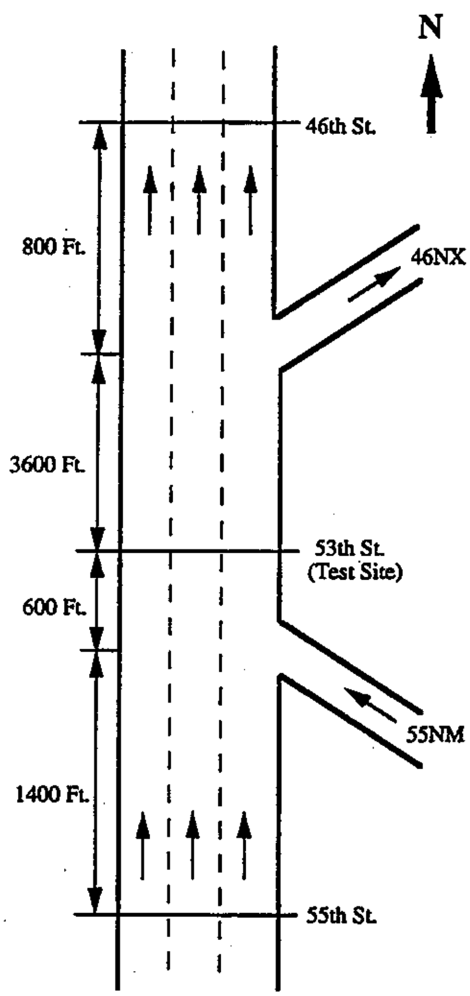

Figure 3. Roadway geometry for entry/exit case.

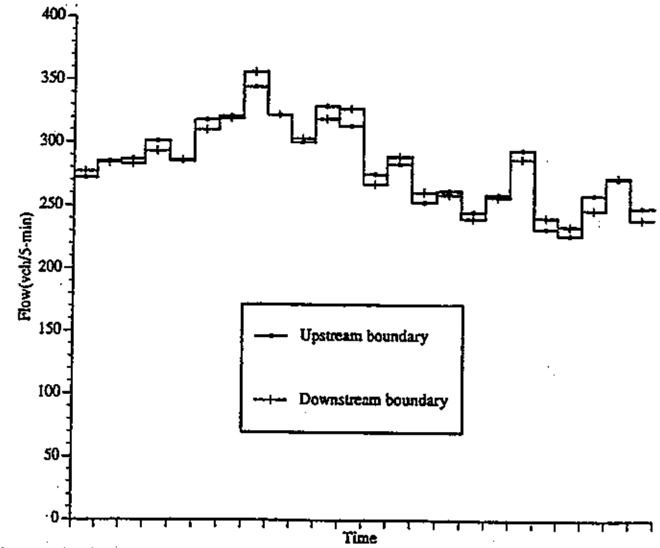

Figure 4. Arrival and departure patterns for uncongested pipeline case.

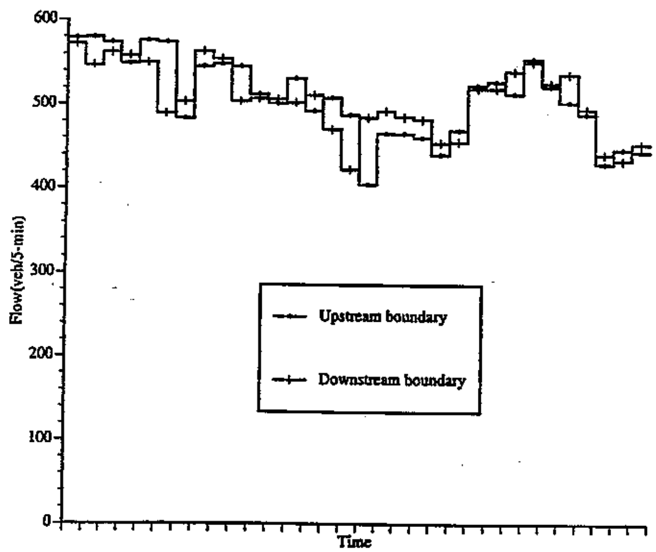

Figure 5. Arrival and departure patterns for congested pipeline case.

departure pattern for the congested pipeline is shown in Figure 5. Observations were recorded at 5 minute intervals over a span of 2 hours and 40 minutes. These field data have also been used in [3,7,10].

In these field data, the congested case represents a road section that changes from uncongested to congested flow and remains congested for approximately 2 hours, then changes from congested to uncongested flow. For each numerical method that we tested, the largest error occurred in the second *congestion-change* interval, where flow changes from congested to uncongested or vice-versa. The next largest error occurred at the first congestion-change interval.

In the implicit methods programs, we used a *large* time step in the intervals where the traffic is congested and we used a *small* time step in congestion-change intervals to minimize the error in these intervals (see also [7]).

4.3. Entry/Exit

The entry/exit freeway case is a section of I-35 W northbound in Minneapolis. The upstream/downstream boundaries were set at the location of 55^{th} Street and 46^{th} Street, respectively. This test case consists of a 6400 ft section of three lane freeway with one entrance ramp and one exit ramp. The entrance ramp is located 1400 ft below the upstream boundary and the exit is located 5600 ft below the upstream boundary. The first check station is located 2000 ft below the upstream boundary; the second check station is located 3800 ft below the upstream boundary. The roadway geometry for the entry/exit case is presented in Figure 3. Data were collected by the Department of Civil Engineering and the Minnesota Department of Transportation on November 8, 1989. The arrival and departure pattern for the entry/exit case is shown in Figure 6. The data consists of flow measurements (vehicles/5 minutes/3 lanes) made at the boundaries and at the check stations and ramp flow measurements (in vehicles/5 minutes) made at each ramp. Observations were recorded at 5 minute intervals during one morning from 6:05 a.m. to 9:30 a.m. The initial conditions were not specified so we have assumed the initial flow to be the average of the flow values at the check stations at 6:05 a.m., and constant along the road section. For this report, only the measurements made at the first check station were used in comparisons with the numerical program output.

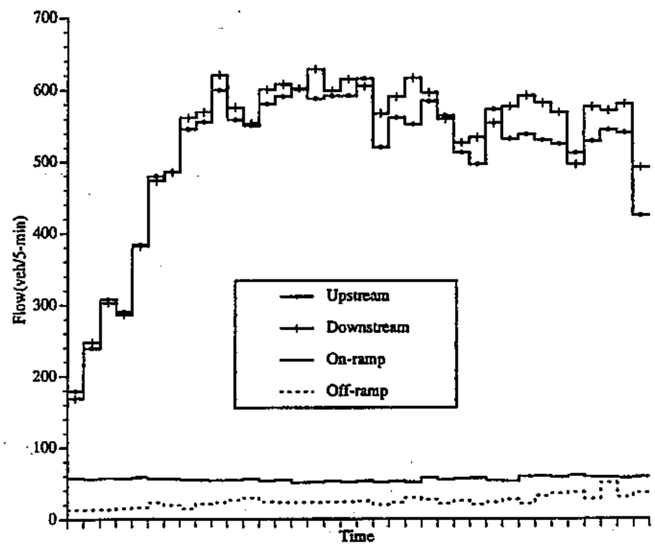

Figure 6. Arrival and departure patterns for entry/exit case.

In this test case, the flow is assumed to be uncongested at all times. Merging flow from the entry ramp is added to the flow at the first node downstream of the ramp. If merging flow plus mainstream flow exceeds the maximum flow $q_{\max}$, the flow value at the entry node is set to $q_{\max}$ and any excess merging flow is not used in the calculations. Exiting flow is subtracted from the first node downstream of the exit ramp. Details of the modelling can be found in [12].

5. RESULTS

The roadway geometry for the uncongested pipeline case, the congested pipeline case, and the entry/exit case are presented in Figures 1–3. The arrival and departure pattern for the uncongested pipeline, the congested pipeline, and entry/exit case are shown in Figures 4–6. Table 1 contains the empirical data to obtain a q-k relation. The error statistics and computer execution times from the uncongested pipeline, congested pipeline, and entry/exit flow cases are summarized in Tables 2–4.

To test the program, the time stepsize selection was made as follows. For the Lax method, we set $\Delta t = 1$ sec. This is required to maintain numerical stability. For the Euler implicit method, the time stepsize was increased such that the maximum error did not exceed that of the Lax method. For the uncongested and entry/exit flow cases, a single time stepsize of $dt = 10$ sec was selected. For the congested flow case, two different time stepsizes were used. One *small* stepsize of $dt = 3$ sec was used in the 5 min time intervals of change from congested to uncongested (or vice versa) and a *large* stepsize of $dt = 6$ sec was in the other time intervals.

Traffic volume and speed comparisons for the uncongested flow case shown in Figures 7–8 indicate that both the Lax and Euler models have about the same level of error (see Table 2). Computer execution time using the Euler implicit method was 5.9 times faster than that using

Table 1. Empirical q-k data.

k = density (veh/mile/lane) q = flow (veh/hour/lane)			
Density	Flow	Density	Flow
0	0	66	2376
10	650	76	2432
20	1260	98	2352
30	1860	124	2232
32	1952	150	1500
35	2100	175	525
36	2124	186	0

Table 2. Results for the uncongested flow case.

Lax $dt = 1$ sec Euler $dt = 10$ sec Execution time (sec), Volume error (veh/5 min), Speed error (miles/hour)					
Method	Execution Time	Volume		Speed	
		Maximum	Average	Maximum	Average
Euler	4.8 sec	10.0	4.0	4.6	3.0
Lax	28.4 sec	9.3	3.6	4.6	3.0

Table 3. Results for the congested flow case.

Lax $dt = 1$ sec Euler $dt = 6 : 3$ sec Execution time (sec), Volume error (veh/5 min), Speed error (miles/hour)					
Method	Execution Time	Volume		Speed	
		Maximum	Average	Maximum	Average
Euler	10.0 sec	65.9	14.5	48.8	8.6
Lax	30.6 sec	102.5	16.8	35.5	7.8

Table 4. Results for the entry/exit flow case.

Lax $dt = 1$ sec Euler $dt = 10$ sec Execution time (sec), Volume error (veh/5 min), Speed error (miles/hour)					
Method	Execution Time	Volume		Speed	
		Maximum	Average	Maximum	Average
Euler	12.7 sec	65.9	11.7	19.9	5.7
Lax	92.8 sec	66.7	11.7	20.4	5.7

the Lax method when simulation used a 4000 ft freeway road section with a total simulation time of 2 hours.

Traffic volume and speed comparisons for the congested flow case are shown in Figures 9–10. In the congested traffic flow situation, the simulation results have the same changing pattern as the field traffic flow data collected at the check station. During congested traffic flow, the speed values of the simulation results were consistently 10 miles/hour lower than that of the observed data. Computer execution time using Euler implicit method was 3.1 times faster than that using the Lax method when simuation used a 3600 ft freeway road section with a total simulation time of 2 hours and 40 minutes. In this congested case, the maximum error produced by the Euler

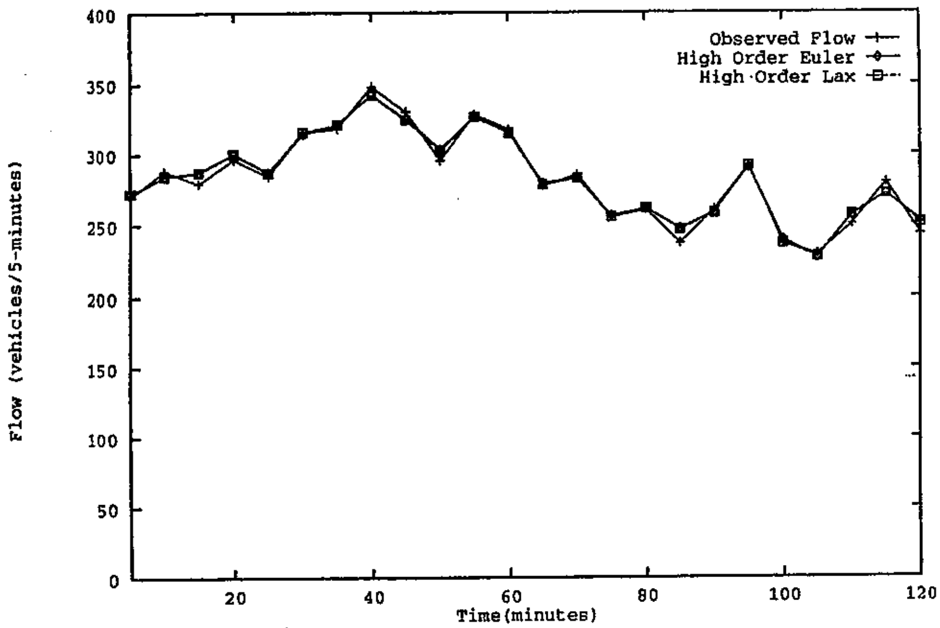

Figure 7. Comparison of volumes for uncongested pipeline case.

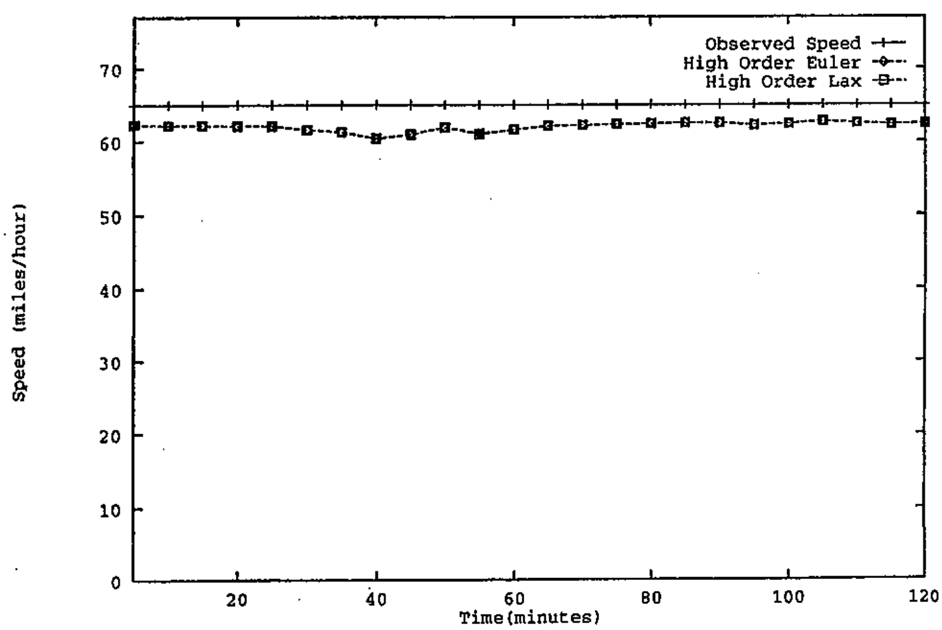

Figure 8. Comparison of speeds for uncongested pipeline case.

method was about half of the maximum error produced by the Lax method. This congested pipeline data was also used for the test of simple continuum model using the Lax and Euler schemes. Our test results show that the maximum traffic volume error using the Euler method and the momentum conservation model (Euler-Momentum) was about four times smaller than that using the Lax method and the simple continuum model, and it was about four times smaller than that using the Euler method and simple continuum model [7].

Traffic volume and speed comparisons for the entry/exit flow case are shown in Figures 11 and 12. The simulation results from the Lax method applied to the momentum conservation model (Lax-Momentum) case and Euler-Momentum case matched very close to those obtained from the upwind scheme applied to the momentum conservation model (see [12]). Volume simulation results were about the same as that of the field data. They followed the changes in traffic demand introduced from the upstream and downstream boundary conditions. Fluctuations in

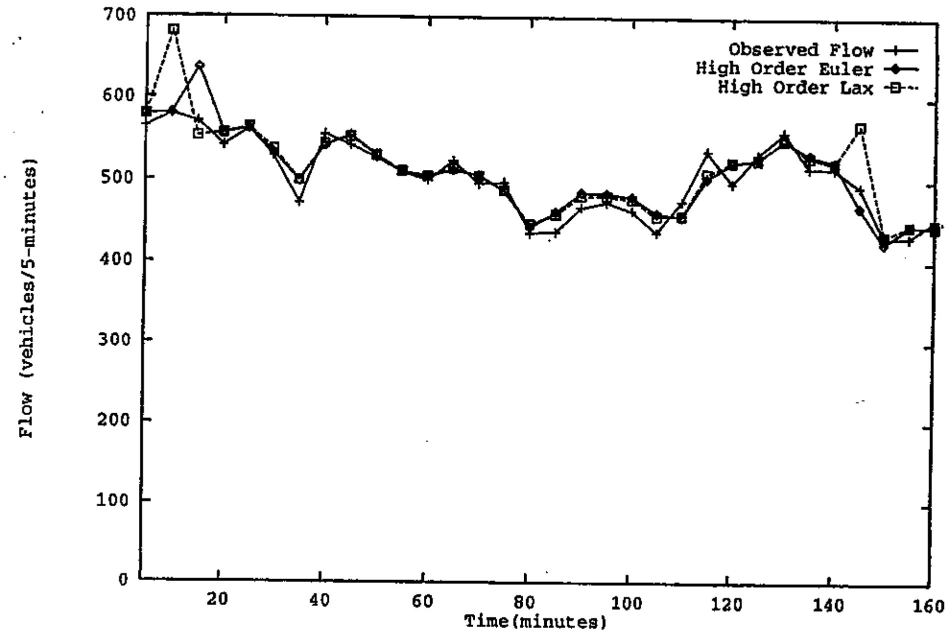

Figure 9. Comparison of volumes for congested pipeline case.

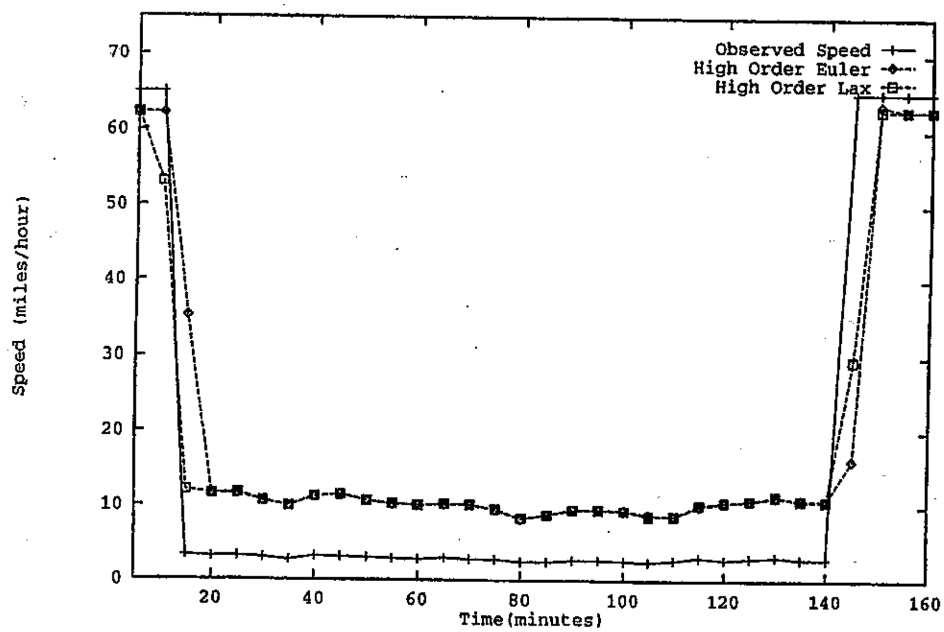

Figure 10. Comparison of speeds for congested pipeline case.

the speed measurements due to congestion were captured by both Lax-Momentum and Euler-Momentum discrete models. Computer execution time using Euler implicit method was about seven times faster than that using the Lax method when simulation used a 6400 ft freeway road section with a total simulation time of 3 hours.

6. CONCLUSIONS

We implemented two high-order continuum models using an explicit (Lax) method and an implicit (Euler) method. We wrote an experimental code in C simulating a freeway (un)congested pipeline and freeway entry/exit traffic flow. Tests with real data collected from the I-35 W freeway in Minneapolis were conducted on a workstation computer. Our tests show that the implicit Euler method provides the same or better accuracy than explicit Lax method in the (un)congested pipeline data case. The implicit Euler method was three times faster than the Lax method in the congested case. If both Euler implicit and Lax explicit method were used

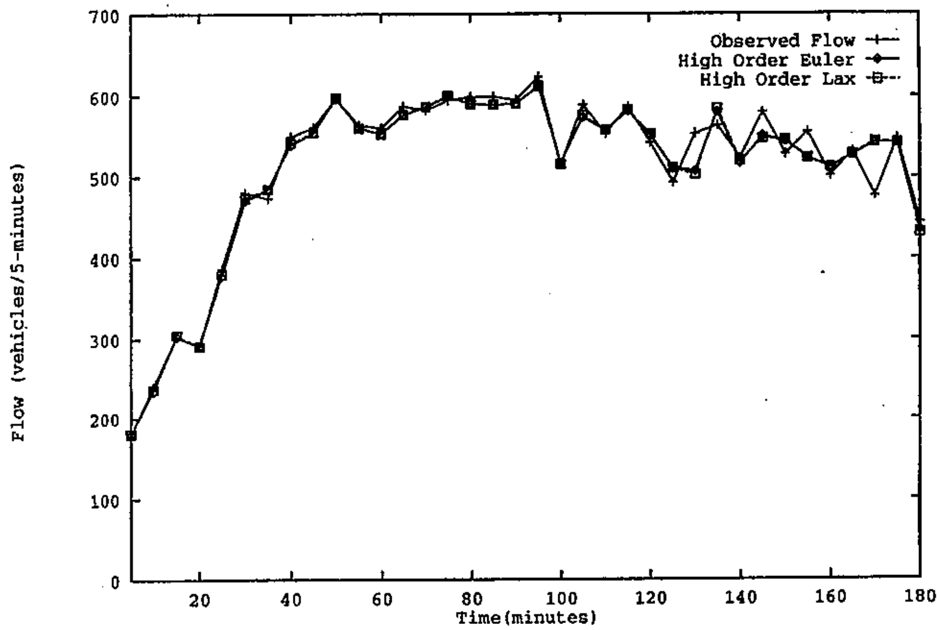

Figure 11. Comparison of volumes for entry/exit case.

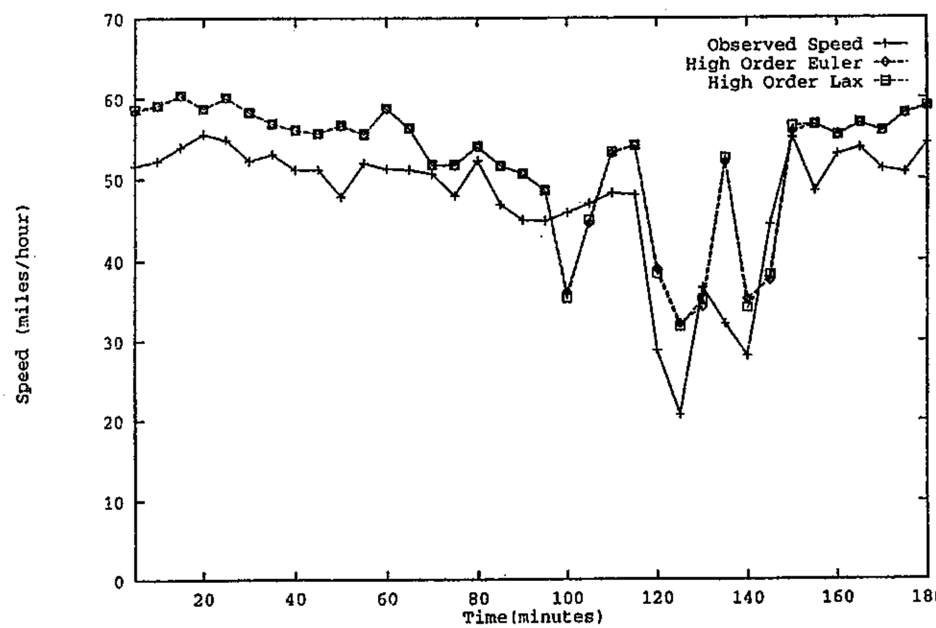

Figure 12. Comparison of speeds for entry/exit case.

to simulate the eight mile stretch of I-35 W freeway section for which we have data, the Euler implicit method is expected to be more efficient than the Lax method.

References

1. M.H. Lighthill and G.B. Witham, On kinematic waves: II A theory of traffic flow on long crowded roads, *Proceed. R. Soc. Ser.* **A 229** (1178), 317–345 (1955).
2. H.J. Payne, Models of freeway traffic and control, *Proceed. Math. of Publ. Syst.* **1** (1), 51–61 (1971).
3. P.G. Michalopoulos, Ping Yi, D.E. Beskos and A.S. Lyrintzis, Continuum modeling of traffic dynamics, In *Proc. of the 2nd Int. Conf. on Appl. of Advanced Tech. in Transportation Eng.*, August 18–21, 1991, pp. 36–40, Minneapolis, Minnesota, (1991).
4. P.G. Michalopoulos and J. Lin, A freeway simulation program for microcomputers, In *Proceed., 1st National Conf. on Microcomputers in Urban Transp.*, pp. 330–341, ASCE, California, (1985).
5. C.J. Leo and R.L. Pretty, Numerical simulation of macroscopic continuum traffic models, *Transportation Research* **26B** (3), 207–220 (1990).

6. C. Hirsch, *Numerical Computation of Internal and External Flows*, Vol. 2, John Wiley and Sons, (1988).
7. A.T. Chronopoulos, P. Michalopoulos and J. Donohoe, Efficient traffic flow simulation computations, *Mathl. Comput. Modelling* **16** (5), 107–120 (1992).
8. B.D. Greenshields, A study of traffic capacity, *Proc. Highway Res. Board* **14**, 448–477 (1934).
9. W. McShane and R. Roess, *Traffic Engineering*, Prentice-Hall, (1990).
10. P.G. Michalopoulos, E. Kwon and J. Kang, Enhancements and field testing of a dynamic freeway simulation program, *Transportation Research Records* (1991) (to appear).
11. J.J. Dongarra *et al.*, *LINPACK User's Guide*, SIAM Publications, (1979).
12. P. Yi, Development and field testing of advanced continuum traffic flow models for congested freeways, Ph.D. Thesis, University of Minnesota, (1992).